

## Factors controlling $^{222}\text{Rn}$ activity of groundwater in Jiroft plain, Iran

M. Faryabi<sup>1\*</sup>, H.R. Mohammadi Behzad<sup>2</sup>, R. Shojaheydari<sup>3</sup>

<sup>1</sup>Department of Ecological Engineering, Faculty of Natural Resources, University of Jiroft, Jiroft, Iran

<sup>2</sup>Chinese Academy of Sciences, Beijing, China

<sup>3</sup>Kerman Regional Water Company, Kerman, Iran

### ► Original article

**\*Corresponding author:**

Mohammad Faryabi, Ph.D.,

E-mail: [faryabi753@yahoo.com](mailto:faryabi753@yahoo.com)

Received: November 2023

Final revised: December 2023

Accepted: February 2024

*Int. J. Radiat. Res., July 2024;*  
22(3): 639-646

DOI: [10.61186/ijrr.22.3.639](https://doi.org/10.61186/ijrr.22.3.639)

**Keywords:** Groundwater,  $^{222}\text{Rn}$ , Spatial analysis, Jiroft plain.

### INTRODUCTION

Radon gas ( $^{222}\text{Rn}$ ) is a radioactive, odorless and colorless gas that occurs naturally in geological environments. This gas has a half-life of about 3.82 days <sup>(1)</sup>.  $^{222}\text{Rn}$  has a very complex behavior in groundwater <sup>(2)</sup>. Several factors affect the behavior and concentration of radon in groundwater. The concentration of radon gas in groundwater is a function of the uranium content of rocks (parent radionuclides such as  $^{238}\text{U}$ ,  $^{232}\text{Th}$ , and  $^{226}\text{Ra}$ ) and geological structures (faults and lineaments) <sup>(3)</sup>. Rocks such as shale, granite, syenite, pegmatite, and gneiss increase the concentration of radon gas in groundwater <sup>(4)</sup>. Phosphate-rich sedimentary rocks and fluvial sandstone are also important sources of radon <sup>(5,6)</sup>. Carbonate rocks and their sediments have a low uranium content <sup>(7,8)</sup>. Faults and fractures increase the permeability of bedrock and facilitate the movement of radon gas <sup>(9)</sup>.  $^{222}\text{Rn}$  can easily travel long distances through fractures, pores, and voids <sup>(10)</sup>. The physical properties of bedrock and soil and the size of soil grains also affect the concentration of radon gas <sup>(11-13)</sup>. The mixing of groundwater with different origins and the residence time of groundwater change  $^{222}\text{Rn}$  concentration <sup>(14)</sup>. The processes such as advection and diffusion introduce  $^{222}\text{Rn}$  to the groundwater system. Atmospheric loss is also the most important process that removes  $^{222}\text{Rn}$  from aquatic systems <sup>(15)</sup>.

### ABSTRACT

**Background:** Radon gas concentration in water has received increasing attention due to its adverse effects on human health. Several factors affect the behavior and nature of this gas in aquatic systems. This study aimed to investigate factors governing the spatial variations of  $^{222}\text{Rn}$  in the groundwater of the Jiroft plain, Iran.

**Materials and Methods:** Water samples were collected from abstraction wells to analyze  $^{222}\text{Rn}$  and the physicochemical properties of groundwater.  $^{222}\text{Rn}$  activity was measured using a RAD 7 instrument.

**Results:**  $^{222}\text{Rn}$  concentration of the groundwater ranged from 5.83 to 34.55 Bq/l. The  $^{222}\text{Rn}$  activity was larger than the permissible limit of the United States Environmental Protection Agency in many cases.

**Conclusion:** Hydrogeological factors, such as depth to water, bedrock situation, aquifer transmissivity, and fault activity, had a good relationship with the spatial variation of  $^{222}\text{Rn}$ . No significant relationship was observed between  $^{222}\text{Rn}$  concentration and physicochemical parameters of groundwater.

In recent years, several studies have been conducted on the measurement of radon gas concentration in groundwater and its health risks. Malakootian *et al.* <sup>(4)</sup> reported a concentration of  $^{222}\text{Rn}$  gas between 0 and 18.48 Bq/l in the villages around the RafaSANJAN fault. Asadi Mohammad Abadi *et al.* <sup>(3)</sup> measured the concentration of radon gas in 33 groundwater samples around the Anar fault. The results of their research showed that the activity of  $^{222}\text{Rn}$  varied between 1.33 and 29.91 Bq/l. Sukanya *et al.* <sup>(2)</sup> investigated  $^{222}\text{Rn}$  concentration in the groundwater of southeastern Punjab, India. They stated that the concentration of radon gas can be controlled by a variety of geochemical reactions and surface processes. Fouladi-Fard *et al.* <sup>(16)</sup> investigated the concentration of radon gas in drinking water wells of Qom province, Iran, and found a lower radon concentration than the WHO (World Health Organization) permission limit in all samples. Han *et al.* <sup>(1)</sup> measured the radon content of water and brackish groundwater in Jeju, Korea, and introduced the residence time of groundwater and geological conditions as the main factors controlling spatial variations of  $^{222}\text{Rn}$ . Doung *et al.* <sup>(17)</sup> studied radon activity near uranium mines in northern Vietnam and showed that the  $^{222}\text{Rn}$  content of springs in the dry season was higher than in the wet season. This condition was attributed to the leakage of radon from the uranium mines into the spring water.

According to the literature, the factors governing

the spatial variations of  $^{222}\text{Rn}$  are still not well understood. Some researchers have examined the relationship between  $^{222}\text{Rn}$  concentration and water quality parameters such as temperature and electrical conductivity. However, the effect of hydrogeological parameters such as aquifer thickness, bedrock depth, aquifer transmissivity, and density of faults on the spatial distribution of radon concentration has not been investigated. Therefore, this study was conducted to elucidate factors influencing the spatial variation of  $^{222}\text{Rn}$  in the groundwater of an alluvial aquifer. This research mainly aimed to investigate the impacts of geological, hydrochemical, and hydrogeological factors on the spatial variations of  $^{222}\text{Rn}$  in the groundwater of the Jiroft plain, southeastern Iran.

## MATERIALS AND METHODS

### Study area

The Jiroft plain, with an area of about 1405 Km<sup>2</sup> and a semi-arid climate with an average annual rainfall of 170 mm<sup>(18)</sup>, is located in the southeast of Iran. Agricultural lands are the most important land use of the area. The Jiroft plain is located in a tectonically active area, where the impact of tectonic forces has caused faults and fractures. The eastern Sabzevaran fault, the western Sabzevaran fault, and the Dalfard fault are the most important faults in the study area. There are various geological units in this plain (figure 1). Igneous rocks, including granite and rhyolite, are outcropped in the northeastern margin of the plain. Regional metamorphic rocks (amphibolite facies) are observed in the western part. Marl, shale, sandstone, and conglomerate are also the most important sedimentary rocks, which often outcrop in the western half of the plain. The most important geological unit of the region is alluvial sediments, which cover a vast part of the plain and have created a good groundwater reservoir (aquifer).

### Study method

A total of 30 water samples were collected from abstraction wells in March 2020. The locations of the sampling stations are shown in figure 1. Electrical conductivity (EC), temperature, and pH were measured at the field using a portable EC meter (HACH HQ40D, Germany). Water samples were analyzed in the laboratory of the Kerman Graduate University of Technology, Iran. Major ions, including calcium ( $\text{Ca}^{2+}$ ), magnesium ( $\text{Mg}^{2+}$ ), sodium ( $\text{Na}^+$ ), chloride ( $\text{Cl}^-$ ), and sulfate ( $\text{SO}_4^{2-}$ ), were determined by the ion chromatography method (using Metrohm 761 Compact IC, Germany). The bicarbonate ion ( $\text{HCO}_3^-$ ) was determined by the titration method.  $^{222}\text{Rn}$  concentration was measured using a RAD 7 instrument (DURRIDGE Company, United States of America). RAD 7 is an active detector that works based on the amount of alpha particles emitted from

radon gas<sup>(19)</sup>. The results of the analysis of water samples were interpreted using bivariate diagrams of qualitative parameters and different spatial distribution maps.

### Statistical analysis

In this study, Minitab software (Minitab Company, USA) was used to check the statistical distribution of  $^{222}\text{Rn}$ . The frequency distribution histogram was used to this purpose. Arc GIS software (ESRI Company, USA) was used to investigate the effect of various hydrogeological parameters on the spatial distribution of  $^{222}\text{Rn}$ . The Pearson correlation coefficients between different parameters and the spatial variability of  $^{222}\text{Rn}$  were calculated using the spatial analysis toolbox of Arc GIS.

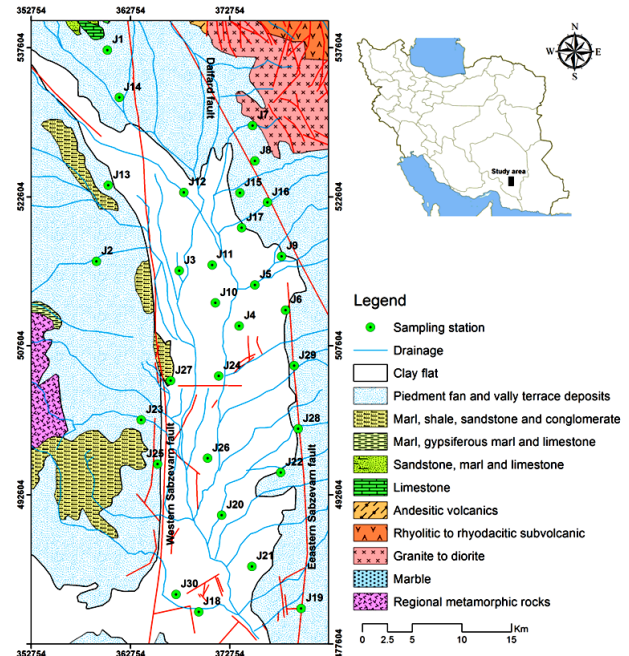


**Figure 1.** Geological map of the study area and location of sampling stations.

## RESULT

Table 1 presents the results of the analysis of groundwater samples, indicating that the concentration of  $^{222}\text{Rn}$  ranges from  $5.83 \pm 0.01$  to  $34.55 \pm 0.85$  Bq/l with an average of  $19.55 \pm 0.73$  Bq/l. The lowest and the highest concentrations of  $^{222}\text{Rn}$  were measured in samples J28 and J30, respectively. The histogram of the  $^{222}\text{Rn}$  frequency distribution (figure 2) showed a  $^{222}\text{Rn}$  concentration of 18-20 Bq/l for the largest numbers of samples.  $^{222}\text{Rn}$  concentrations of groundwater followed a normal distribution (figure 2). The pH of water samples varied between 6.9 and 8.4, suggesting the alkaline environment of the groundwater system. The temperature of groundwater ranged from 22.7 to 32.3 °C. The lowest and the highest temperatures corresponded to the samples J24 and J19,

respectively. The average electrical conductivity of groundwater samples was 1036.8  $\mu\text{S}/\text{cm}$ , ranging from 434 to 5260  $\mu\text{S}/\text{cm}$ . The highest amounts of electrical conductivity, sodium ion, and chloride ion were recorded in the sample J25. The highest concentrations of calcium, magnesium, and sulfate ions were observed in the sample J20. The sample J28

contained the highest concentration of bicarbonate ions. The above-mentioned information indicated that the quality of groundwater can be affected by different processes such as the dissolution of halite ( $\text{NaCl}$ ), gypsum ( $\text{CaSO}_4$ ), and anhydrite ( $\text{CaSO}_4 \cdot 2\text{H}_2\text{O}$ ), as well as recharge by good-quality waters (a low EC and a high bicarbonate).

**Table 1.** Physicochemical characteristics of water samples (pH: Acidity, EC: Electrical Conductivity, Ca: Calcium, Mg: Magnesium, Na: Sodium,  $\text{HCO}_3$ : Bicarbonate, Cl: Chloride,  $\text{SO}_4$ : Sulphate).

Sample ID	$^{222}\text{Rn}$	pH	Temperature	EC	Ca	Mg	Na	$\text{HCO}_3$	Cl	$\text{SO}_4$
	Bq/l		°C							
J1	11.28 ± 0.21	8.00	-	580	2.5	1	2.4	2.5	1.2	2.2
J2	21.11 ± 1.58	7.15	25.1	642	2.9	1.5	2.2	3.1	1.4	2.1
J3	27.15 ± 1.12	7.48	24.5	1123	2.6	2.5	7.1	4.7	2.5	5
J4	7.32 ± 0.05	7.60	-	550	1.6	0.9	3.1	2.5	1.5	1.6
J5	10.76 ± 0.58	7.59	28.3	644	0.5	0.8	5.2	1.7	2.3	2.5
J6	19.67 ± 0.78	7.55	31.1	642	1.6	0.5	4.2	1.8	2.2	2.3
J7	20.88 ± 0.65	8.40	-	475	1	1	2.7	2	1	1.7
J8	31.21 ± 1.73	8.00	-	560	1.01	1	2.67	2.1	1	1.71
J9	28.31 ± 0.32	7.49	28	455	1.7	0.4	2.2	2.4	0.5	1.4
J10	15.85 ± 0.09	7.48	24.5	1123	2.6	2.5	7.1	4.7	2.5	5
J11	18.41 ± 0.12	7.80	25	553	0.7	1	4.1	2.8	1.6	1.4
J12	26.14 ± 0.54	7.40	25.3	1083	3.7	3.1	4.8	3.8	2.9	4.9
J13	18.9 ± 0.23	7.20	23.7	1027	3.7	2.6	5.1	4.4	2	5
J14	19.52 ± 0.26	7.15	25.1	642	2.9	1.5	2.2	3.1	1.4	2.1
J15	24.98 ± 1.32	7.24	27.2	836	2.6	1.6	4.5	3.7	2.4	2.6
J16	30.67 ± 1.02	7.49	28	455	1.7	0.4	2.2	2.4	0.5	1.4
J17	23.12 ± 0.13	7.50	-	600	2	2	2	3.5	0.6	1.9
J18	28.11 ± 0.65	7.90	-	840	1.5	0.9	6.2	2.5	3	3.1
J19	9.08 ± 0.05	7.23	32.3	2840	11	1.8	16.6	2.1	18	9.3
J20	13.07 ± 0.43	7.22	26	3340	21.8	8.2	15.7	4.3	4	37.4
J21	17.71 ± 0.54	7.75	-	1122	1.75	1.25	7.9	3.25	4.35	3.3
J22	6.54 ± 0.01	8.02	30.5	822	1	0.3	7	2.2	2.7	3.4
J23	23.59 ± 0.21	8.20	27	462	0.8	0.5	3.4	2.3	0.9	1.5
J24	10.34 ± 0.03	7.84	22.7	550	1.9	1	2.4	2.5	1.2	1.6
J25	23.74 ± 0.61	7.30	28.3	5260	13	7.8	32.7	4	28.4	21.1
J26	14.62 ± 1.13	7.88	23.5	434	1.2	0.6	2.3	2.4	1.1	0.6
J27	31.97 ± 1.62	8.20	27	462	0.8	0.5	3.4	2.3	0.9	1.5
J28	5.83 ± 0.01	6.90	26.1	1678	4.1	2.4	12.8	8.1	4.7	6.5
J29	9.74 ± 0.13	7.30	26	477	2.5	1.2	1.4	2.7	0.9	1.5
J30	34.55 ± 0.85	7.69	-	825	1.5	1	5.9	3	2.2	3.2

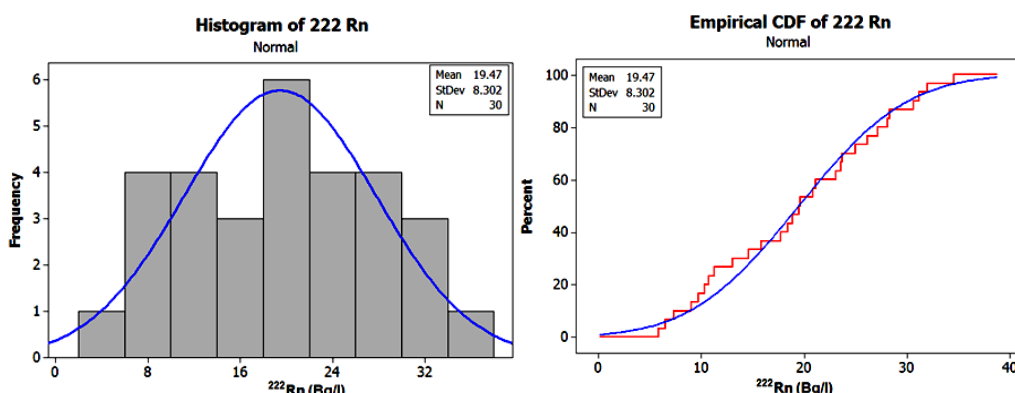


**Figure 2.** Statistical distribution of radon concentration: a frequency histogram, and b cumulative frequency (CDF).

Figure 3 shows the spatial variations of  $^{222}\text{Rn}$  concentration, indicating an increase in  $^{222}\text{Rn}$  activity from the southeast and northwest of the plain to its center and south. The concentration of  $^{222}\text{Rn}$  was larger than the permissible limit (11.1 Bq/l) of the

USEPA (United States Environmental Protection Agency) in a vast part of the study area. Only 26.7% of water samples (J1, J4, J5, J19, J22, J24, J28, and J29) had a concentration lower than the permissible limit of USEPA.

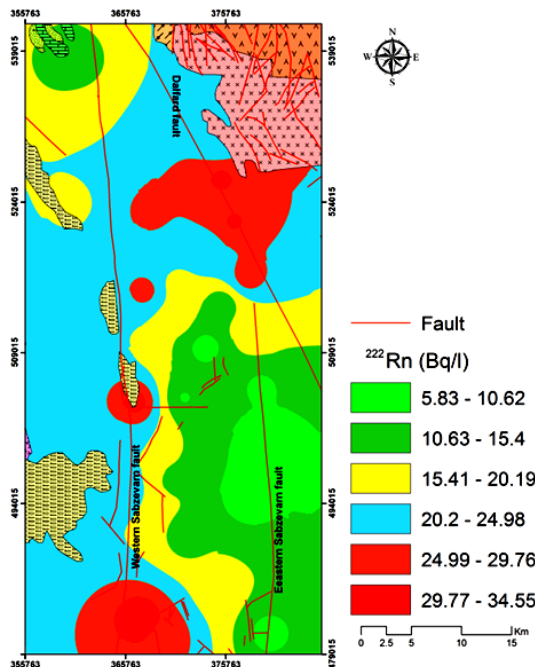


**Figure 3.** Spatial distribution of  $^{222}\text{Rn}$  activity in groundwater of Jiroft plain.

### Possible factors affecting the concentration of $^{222}\text{Rn}$

#### Hydrogeological factors

The spatial distribution of  $^{222}\text{Rn}$  concentration in groundwater system is affected by various factors. Local geology is among the most important factors (20,21). Previous studies showed that the groundwater moves through granite rocks and their sediments contain high concentrations of radon (22). Among sedimentary rocks, shale and sandstone have a good ability to increase the radon content of groundwater (6). As mentioned in the previous sections, the most important geological units of the Jiroft plain include granite and volcanic rocks in the northeast, sedimentary rocks (marl, shale, and sandstone) in the western half, and metamorphic rocks in the southwest. These geological units are the most important factors controlling the type of sediments in the plain. One of the areas that show the highest concentration of  $^{222}\text{Rn}$  in the Jiroft plain is located in the northeast. The presence of granite rocks and their sediments is an important factor in increasing  $^{222}\text{Rn}$  concentration in these areas. The outcrops of shale, sandstone, and their resulting sediments in the western half of the plain have also increased the concentration of  $^{222}\text{Rn}$  in groundwater. The type and depth of bedrock affect the radon concentration of groundwater (2). The aquifer bedrock is of shale type in the western part of the plain. In the central part, conglomerate and sandstone form the bedrock. Limestone rocks are also placed under the conglomerate and recharge the aquifer in the eastern part (23). Spatial variations of the bedrock type affect the  $^{222}\text{Rn}$  activity. The map of bedrock depth is presented in figure 4a (23), showing a variation of 39

and 162 m in the depth of bedrock. The bedrock is deeper in the central part of the plain. This situation can increase the residence time of groundwater and decrease its radon content. It seems that there is an inverse relationship between the bedrock depth and the concentration of  $^{222}\text{Rn}$ . This hypothesis was examined by calculating the correlation coefficient between the map of the bedrock depth (figure 4a) and the spatial distribution map of  $^{222}\text{Rn}$  concentration (figure 3) using the Spatial Analysis package of ArcGIS 10.7 software. As seen in table 2, the correlation coefficient of these layers is -0.41, which confirms the inverse relationship between the depth of the bedrock and the  $^{222}\text{Rn}$  concentration. From hydrologists' viewpoints, the vertical distance between the groundwater table and the bedrock is considered the thickness of the aquifer. Figure 4b indicates the spatial variations of the aquifer thickness, showing that the aquifer is thicker in the central part of the plain. The lowest thickness of the aquifer is seen in the western half. It can be claimed that the concentration of  $^{222}\text{Rn}$  has an inverse relationship with the aquifer thickness ( $R = -0.31$ , table 2).

Waters that can potentially have high radon concentrations are usually shallow and contemporary groundwater (24). The map of depth to groundwater is presented in figure 4c. This map was prepared using the data of water depth in observation wells. These data were prepared by the Kerman Regional Water Authority (KRWA) (25). As seen in figure 4c, the depth of groundwater is more than 27 m in the northwest and southeast of the plain. However, the groundwater depth decreases in other areas (especially in the western half of the plain). According to table 2, the groundwater depth and the  $^{222}\text{Rn}$  concentration have an inverse relationship ( $R = -0.49$ ).

Figure 4d shows the aquifer transmissivity map of the Jiroft plain. Transmissivity is the ability of an aquifer to transfer water through itself. The aquifer transmissivity ranged from 100 to 3460  $\text{m}^2/\text{d}$  in the study area (25). As seen in figure 4d, the aquifer transmissivity decreases from the north to the south of the plain. This pattern of aquifer transmissivity has a direct relationship with the  $^{222}\text{Rn}$  activity ( $R = 0.39$ , table 2).

The presence of faults and their activity affect the spatial variations of  $^{222}\text{Rn}$ . Displacement of rock masses occurs around active faults. As a result of these displacements, many small cracks are gradually created in the rocks (26). These cracks facilitate the migration of radon gas. This situation increases the concentration of radon in the groundwater around the active faults (27). As seen in figure 3, the highest concentration of  $^{222}\text{Rn}$  was measured around the western Sabzevaran fault and the Dalfard fault, where the groundwater is at a lower depth. The concentration of  $^{222}\text{Rn}$  around the eastern Sabzevaran fault is lower than that of the other two main faults

(the western Sabzevaran fault and the Dalfard fault). The most important reason for this issue is the increase in the groundwater depth, the thickness of the aquifer, and the residence time of groundwater. The activity of the eastern Sabzevaran fault is also less than the other two main faults (28). Maps of the

distance to the fault and the fault density are presented in figure 5a and figure 5b, respectively. According to table 2, the concentration of  $^{222}\text{Rn}$  has an inverse relationship with the distance to the fault and a direct relationship with the fault density.

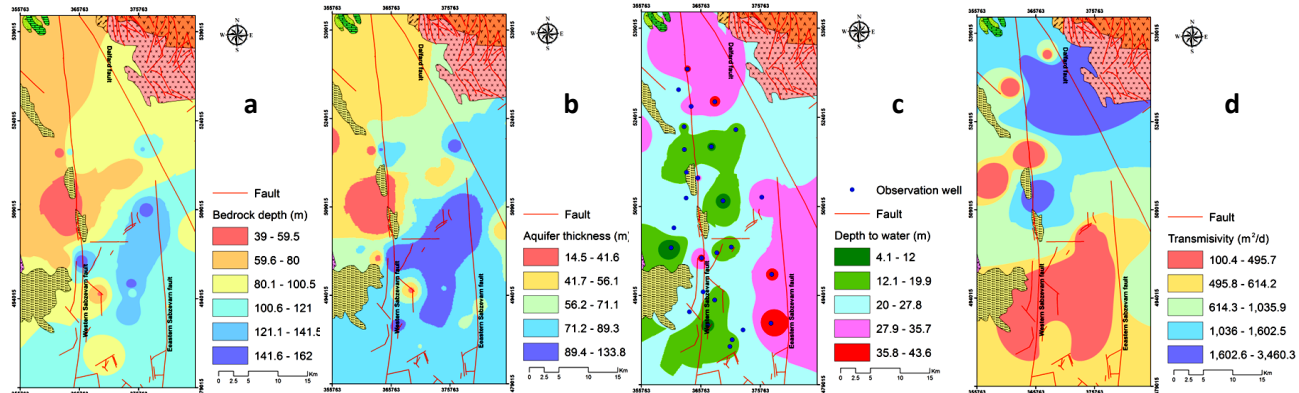


Figure 4. Spatial distribution of **a** Bedrock depth, **b** Aquifer thickness, **c** Depth to the water (July 2020), and **d** Aquifer transmissivity.

Table 2. Results of the statistical analysis using the Spatial Analysis package of Arc GIS.

Layer (map)	Minimum	Maximum	Mean	Standard deviation	Correlation coefficient with $^{222}\text{Rn}$
$^{222}\text{Rn}$	5.83	34.55	19.69	5.12	1
Depth to water	4.13	43.62	24.8	5.11	-0.49
Aquifer transmissivity	100.4	3460.2	1004.9	621.7	0.39
Bedrock depth	39.02	161.98	92.37	17.55	-0.41
Aquifer thickness	14.46	133.76	67.57	17.07	-0.31
Distance to fault	0.00	10316.1	2460.2	2185.44	-0.12
Fault density	0.00	2.88	0.20	0.36	0.21

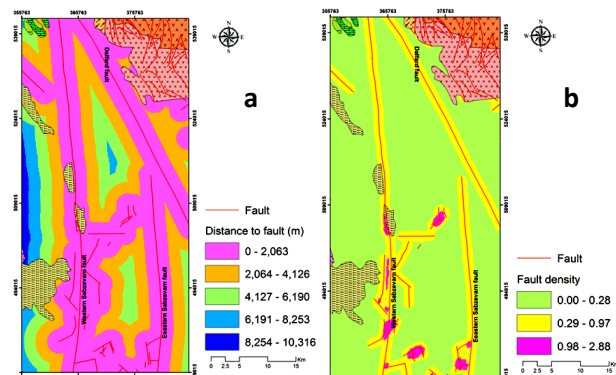


Figure 5. Map of **a** Distance to the fault, and **b** Fault density.

### Hydrochemical factors

The chemical nature of water and its temperature affect the rate of radon dissolution (29). The solubility of radon gas has an inverse relationship with temperature (30). Figure 6 shows the variations of  $^{222}\text{Rn}$  versus the temperature of the groundwater samples. The general trend in this figure is a decrease in  $^{222}\text{Rn}$  concentration with increasing temperature ( $R = -0.07$ ). Nonetheless, three detailed patterns can be identified in figure 6. According to these patterns, groundwater samples are placed into three groups. The first group (group 1) includes samples J2, J3, J10, J11, J12, J13, J14, J24, and J26, which are mainly located in the northern and central parts of the Jiroft plain. The temperature of these samples varies between 22 and 26°C. In group 1, the  $^{222}\text{Rn}$  activity

increases with the increase in groundwater temperature ( $R = 0.72$ ). The second group (group 2) includes samples J6, J9, J15, J16, J23, J25, and J27. In this group, radon activity decreased with increasing temperature ( $R = -0.62$ ). The temperature of these samples ranged from 26 to 32°C. Group 2 samples are mainly located near the western Sabzevaran fault and the Dalfard fault. Samples J5, J19, J20, J22, J28, and J29 are placed in the third group (group 3). There is no strong relationship between  $^{222}\text{Rn}$  variations and temperature ( $R=-0.2$ ). These samples are mainly located around the eastern Sabzevaran fault. According to figure 4, it can be concluded that the mixing of groundwater with different origins occurs in the aquifer. This mixing process can affect the spatial variations of radon concentration. The bivariate plots of  $^{222}\text{Rn}$  versus other groundwater quality parameters are presented in figure 7. As seen in this figure, there are no strong correlations between  $^{222}\text{Rn}$  variation and groundwater quality parameters.

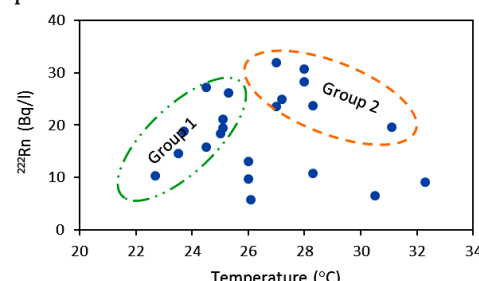
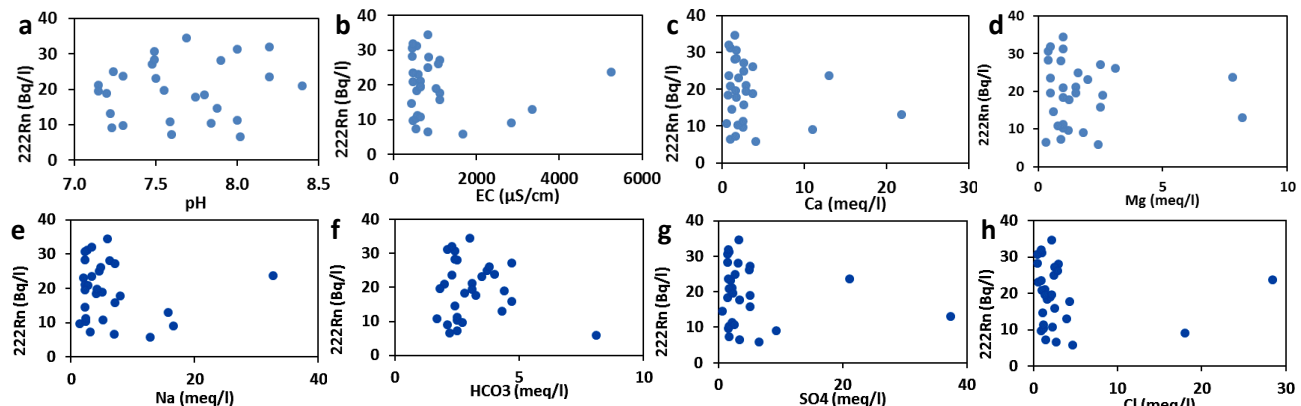


Figure 6. Plot of  $^{222}\text{Rn}$  versus temperature.



**Figure 7.** Bivariate diagram of  $^{222}\text{Rn}$  versus **a** Acidity (pH), **b** Electrical Conductivity (EC), **c** Calcium (Ca), **d** Magnesium (Mg), **e** Sodium (Na), **f** Chloride (Cl).

## DISCUSSION

The concentration of  $^{222}\text{Rn}$  varied between 5.83 and 34.55 Bq/l in the Jiroft plain. The radon concentration values measured in this research are different from the radon concentration reported in similar studies (table 3). These differences could be due to differences in geological and hydrogeological conditions. Radon concentration follows a normal distribution in the study area. Fouladi-Fard *et al.* (16) also reported the normal distribution of  $^{222}\text{Rn}$  in the groundwater of Qom province, Iran. But, Sukanya *et al.* (2) reported a log-normal distribution for  $^{222}\text{Rn}$  data in Punjab, India.

**Table 3.**  $^{222}\text{Rn}$  concentration in alluvial aquifers

Country/ region	Range of $^{222}\text{Rn}$ activity (Bq/l)	Reference
Korea/ Jeju	0.4 – 20.65	(1)
Iran/ Anar	1.33 – 29.91	(3)
Iran/ Rafsanjan	0.00 – 18.48	(4)
India/ Punjab	0.62 – 3.21	(31)
Kenya/ Kericho	4.6 – 22.5	(32)
Saudi Arabia	0.01 – 67.4	(33)
Nigeria/ Ibadan	0.08 - 14.8	(34)

Parameters such as local geology, type and depth of bedrock, aquifer thickness, groundwater depth, aquifer transmissivity, distance to fault, and density of faults control the spatial variations of  $^{222}\text{Rn}$  activity in the study area. Rocks such as granite, shale, and amphibolite have the potential to increase the radon concentration of groundwater in the Jiroft plain. Ameho *et al.* (35) reported the geological factor as one of the factors affecting the radioactivity of groundwater. Mehnati *et al.* (36) have mentioned the effect of granitic rocks on the concentration of radon gas of hot springs in Kerman province, Iran. Cho *et al.* (37) also reported high levels of radon in granite aquifers of South Korea. Oni *et al.* (34) and Sukanya *et al.* (2) have pointed out the effect of bedrock type and depth on  $^{222}\text{Rn}$  concentration.

There is an inverse relationship between the groundwater depth and the  $^{222}\text{Rn}$  concentration in the Jiroft plain. Fouladi-Fard *et al.* (16) reported the inverse relationship of  $^{222}\text{Rn}$  and groundwater depth

in the Qom province, Iran. But Sukanya *et al.* (2) did not find a strong relationship between water depth and  $^{222}\text{Rn}$  activity in hard rocks of southeastern India. Because, the lineaments are the most important factor determining the groundwater potential and its radon content of hard rock formations.

Water mixing is one of the processes affecting radon activity in Jiroft plain. Przylibski and Zebrowski (38) have also emphasized the effect of the mixing process on the radon concentration of the groundwater in southwestern Poland.

The activity of the western Sabzevaran fault and the Dalfard fault has caused high radon anomalies. Sukanya *et al.* (2) investigated the role of fault activity on the spatial variation of the  $^{222}\text{Rn}$  in southeast India. These researchers showed that the activity of faults has increased the concentration of  $^{222}\text{Rn}$ . Li *et al.* (39) also stated that there is a direct relationship between fault activity and radon concentration in central China.

No strong correlation was observed between  $^{222}\text{Rn}$  activity and groundwater quality parameters in Jiroft plain. Studies by Srilatha *et al.* (40), Sharma *et al.* (31), and Sukanya *et al.* (2) also confirm this finding.

To generalize the factors affecting the spatial distribution of radon gas in groundwater of Jiroft plain, the plot of  $^{222}\text{Rn}$  concentration versus the distance to the fault was used (figure 8). Mehrabi (19) showed that the impact of the Jiroft plain faults on the radon concentration was significant up to a distance of 1000 m. Based on this finding and a threshold of 20 Bq/l for  $^{222}\text{Rn}$  (figure 8), the processes affecting the variability of  $^{222}\text{Rn}$  in the groundwater can be expressed as follows:

### A. Proximity to active faults

The samples located in region A (figure 8) have high  $^{222}\text{Rn}$  concentrations ( $> 28 \text{ Bq/l}$ ) and are located close to the Dalfard fault and the western Sabzevaran fault. Therefore, this high concentration of  $^{222}\text{Rn}$  is related to the activity of faults.

### B. Groundwater residence time

Groundwater samples with relatively low radon

activity (5 to 15 Bq/l) are placed in region B (figure 8). Although these samples are located close to the eastern Sabzevaran fault, their low radon concentration is due to the less activity of the fault, the greater depth of the groundwater, the greater thickness of the aquifer, and the longer residence time of the groundwater.

### C. Influences of surficial geology and bedrock

The samples that are classed in region C (figure 8) have relatively a high  $^{222}\text{Rn}$  content (20-30 Bq/l) and are located far from faults. The most important factors responsible for this condition are the radon content of surface geological formations and aquifer bedrock. Proximity to buried faults could also be the possible reason for the increase in  $^{222}\text{Rn}$  concentration.

### D. Combination of groundwater mixing and groundwater residence time

In figure 8, region D includes samples that have  $^{222}\text{Rn}$  activity between 5 and 20 Bq/l and are mainly located in the central part of the plain. The mixing of groundwater with different origins, the greater thickness of the aquifer, and the long residence time of groundwater are the most important factors responsible for this condition.

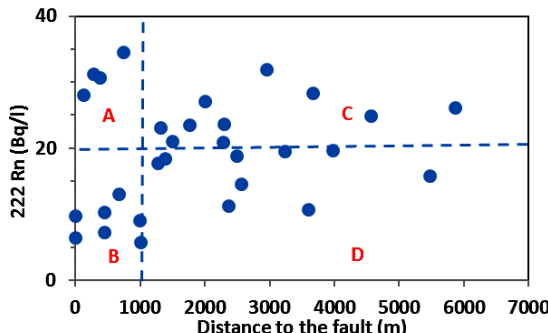


Figure 8. Plot of  $^{222}\text{Rn}$  concentration versus distance to the fault.

## CONCLUSION

This study investigated the factors affecting the spatial distribution of  $^{222}\text{Rn}$  in the groundwater of the Jiroft plain. The concentration of  $^{222}\text{Rn}$  varied between 5.83 and 34.55 Bq/l. Parameters such as groundwater depth, bedrock depth, aquifer thickness, and distance to the fault have inverse relationships with the spatial distribution of  $^{222}\text{Rn}$  concentration. However, aquifer transmissivity and fault density parameters have direct relationships with the spatial variability of  $^{222}\text{Rn}$ . There were no clear relationships between the physicochemical parameters of groundwater and the  $^{222}\text{Rn}$  activity.

## ACKNOWLEDGMENTS

Kerman Graduate University of Technology (KGUT)

is gratefully acknowledged for the chemical analysis of water samples.

**Funding:** None declared.

**Conflicts of interest:** The authors declare no conflicts of interest.

**Ethical consideration:** None.

**Author's contributions:** All authors contributed immensely to the work.

## REFERENCES

1. Han CH, Hong JW, Im HJ (2021) A study of  $^{222}\text{Rn}$  concentration of salty underground water and spring water in Jeju, Korea. *J Radioanal Nucl Chem*, **330**: 563–569.
2. Sukanya S, Noble J, Joseph S (2021) Factors controlling the distribution of radon ( $^{222}\text{Rn}$ ) in groundwater of a tropical mountainous river basin in southwest India. *Chemosphere*, <https://doi.org/10.1016/j.chemosphere.2020.128096>.
3. Asadi Mohammad Abadi A, Rahimi M, Jabbari Koopaei L (2016) The effect of geological structure on radon concentration dissolved in groundwater in nearby Anar fault based on a statistical analysis. *J Radioanal Nucl Chem*, **308**: 801–807.
4. Malakootian M, Khashi Z, Iranmanesh F, Rahimi M (2014) Radon concentration in drinking water in villages nearby Rafsanjan fault and evaluation the annual effective dose. *J Radioanal Nucl Chem*, **302(3)**: 1167–1176.
5. Gundersen LC (1993) The correlation between bedrock geology and indoor radon: where it works and where it doesn't-some examples from the Eastern United States. International Radon Conf. *AARST, Colorado*.
6. Liu H, Wang N, Chu X, Li T, Zheng L, Yan S, Li S (2016) Mapping radon hazard areas using  $^{238}\text{U}$  measurements and geological units: a study in a high background radiation city of China. *J Radioanal Nucl Chem*, **309**: 1209–1215.
7. Gorgoni C, Martinelli G, Sighinolfi GP (1982) Radon distribution in groundwater of the Po sedimentary basin (Italy). *Chem Geol*, **35(3-4)**: 297–309.
8. King PT, Michel J, Moore WS (1982) Ground water geochemistry of  $^{228}\text{Ra}$ ,  $^{226}\text{Ra}$  and  $^{222}\text{Rn}$ . *Geochim Cosmochim Acta*, **46**: 1173–1182.
9. Li C, Su H, Zhang H, Zhou H (2016) Correlation between the spatial distribution of radon anomalies and fault activity in the northern margin of West Qinling Fault Zone, Central China. *J Radioanal Nucl Chem*, **308**: 679–686.
10. Lindsey BD and Ator SW (1996) Radon in groundwater of the lower Susquehanna and Potomac river basins. US Geological Survey water resources investigations report 96e4156, 6. <https://pubs.usgs.gov/wri/1996/4156/report.pdf>. Accessed 20 Jul 2022
11. Choubey VM and Ramola RC (1997) Correlation between geology and radon levels in ground water, soil and indoor air in Bhilangana Valley, Garhwal Himalaya, India. *J Environ Geol*, **32**: 258–262.
12. Ramola RC, Choubey VM, Negi MS (2008) Radon occurrence in soil-gas and groundwater around an active landslide. *Radiat Meas*, **43**: 98–101.
13. Tansi C, Tallarico A, Iovine G, Folino Gallo M, Falcone G (2005) Interpretation of radon anomalies in seismotectonic and tectonic-gravitational settings: the south-eastern Crati graben (Northern Calabria, Italy). *Tectonophysics*, **396(3-4)**: 181–193.
14. Cook PG, Lamontagne S, Berhane D, Clark JF (2006) Quantifying groundwater discharge to Cockburn River, southeastern Australia, using dissolved gas tracers  $^{222}\text{Rn}$  and  $\text{SF}_6$ . *Water Resour Res*, <https://doi.org/10.1029/2006WR004921>.
15. Thiyva C, Chidambaram S, Tirumalesh K, Prasanna MV, Thilagavathi R, Nepolian M (2014) Occurrence of the radionuclides in groundwater of crystalline hard rock regions of central Tamil Nadu, India. *J Radioanal Nucl Chem*, **302**: 1349–1355.
16. Fouladi-Fard R, Amraei A, Fahiminia M, Hosseini MR, Mahvi AH, Omidi Oskouei A, Fiore M, Mohammadbeigi A (2020) Radon concentration and effective dose in drinking groundwater and its relationship with soil type. *J Radioanal Nucl Chem*, **326**: 1427–1435.
17. Duong VH, Vu HD, Nguyen DT, Pham LT, Toth G, Hegedus M, Kovacs T (2023) Seasonal  $^{222}\text{Rn}$  activity in spring water close to rare earth element and uranium mines in North Vietnam. *J Radioanal Nucl Chem*, <https://doi.org/10.1007/s10967-023-08872-x>

18. Faryabi M (2023) A fuzzy logic approach for land subsidence susceptibility mapping: the use of hydrogeological data. *Environ Earth Sci*, <https://doi.org/10.1007/s12665-023-10909-z>.

19. Mehrabi A (2019) Measuring the concentration of radon gas in groundwater of Jiroft plain and its relation with the region faults. *J Nat Environ Hazards*, **8**(21): 267-282.

20. Lam RHF, Brown JP, Fan AM (1994) Chemicals in California drinking water: Source of contamination, risk assessment, and drinking water standards. In: Wang RGM, editor. Water contamination and health: Integration of exposure assessment, toxicology, and risk assessment. New York: Marcel Dekker, Inc15-44.

21. Friedmann H, Baumgartner A, Bernreiter M, Graser J, Gruber V, Kabrt F, Kaineder H, Maringer FJ, Ringer W, Seidel C, Wurm G (2017) Indoor radon, geogenic radon surrogates and geology-investigations on their correlation. *J Environ Radioact*, **166**(2): 382-389.

22. Hess CT, Michel J, Horton TR, Prichard HM, Coniglio WA (1985) The occurrence of radioactivity in public water supplies in the United States. *Health Phys*, **48**(5): 553-86.

23. Abkav-Louis Berger (1976) Ground water and agricultural feasibility study Jiroft - Minab project. Abkav-Louis Berger Consulting Engineers.

24. Przylibski TA (2011) Shallow circulation groundwater – the main type of water containing hazardous radon concentration. *Nat Hazards Earth Syst Sci*, **11**: 1695-1703.

25. KRWA (2020) Report of groundwater study of Jiroft plain. *Kerman Regional Water Authority*

26. Ghosh D, Deb A, Sengupta R (2009) Anomalous radon emission as precursor of earthquake. *J Appl Geophys*, **69**(2): 67-81

27. Lawrence E, Poeter E, Wanty R (1991) Geohydrologic, geochemical and geologic controls on the occurrence of radon in groundwater near Conifer, Colorado USA. *J Hydrol*, **127**(1): 367-386

28. Shafei Bafti A, Jafari HR, Shahpasandzadeh M (2009) Dynamic tectonics and earthquake hazard estimation in Sabzevaran region. *Geotech Geol*, **5**(3): 229-238

29. El-Araby EH, Soliman HA, Abo-Elmagd M (2019) Measurement of radon levels in water and the associated health hazards in Jazan, Saudi Arabia. *J Radiat Res Appl Sci*, **12**(1): 31-36.

30. Kulalı F, Akkurtlu I, Özgür N (2016) Investigation of the radon levels in groundwater and thermal springs of Pamukkale region. *Acta Phys Pol*, **130**(1): 496-498.

31. Sharma D, Keesari T, Rishi M, Thakur N, Pant D, Vasant Mohokar H, Jaryal A, Kamble SN, Kumar Sinha U (2020) Radiological and hydrological implications of dissolved radon in alluvial aquifers of western India. *J Radioanal Nucl Chem*, **323**: 1257-1267.

32. Rotich CK, Hashim NO, Chege MW, Nyambura C (2020) Measurement of radon activity concentration in underground water of bureti sub-county of Kericho county Kenya. *Radiat Protect Dosim*, **192** (1): 56-60.

33. Alabdula'aly AI (2014) Occurrence of radon in groundwater of Saudi Arabia. *J Environ Radioact*, **138**: 186-191

34. Oni E, Oladapo O, Aremu A (2022) Preliminary probe of radon content in drinking water in Ibadan, south-western Nigeria. *Int J Radiat Res*, **20** (4): 871-877.

35. Ameho E, Kpegle D, Glover E, Adukpo O, Sulemana A, Agalga R, Kpordzro R, Quarshie E, Hogarh JN (2023) Naturally occurring radioactive material in groundwater: potential health risk to the inhabitants at Osino in the eastern region of Ghana. *Int J Radiat Res*, **21**(4): 779-787.

36. Mehnati P, Doostmohammadi V, Jomehzadeh A (2022) Determination of Rn- 222 concentration and annual effective dose of inhalation in the vicinity of hot springs in Kerman province, southeastern Iran. *Int J Radiat Res*, **20**(1): 211-216.

37. Cho BW, Hwang JH, Lee BD Lee, Oh YH, Choo CO (2020) Radon concentrations in raw water and treated water used for bottled water in South Korea. *Sustainability*, **12**: 5313.

38. Przylibski TA and Zebrowski A (1999) Origin of radon in medicinal waters of Ladek Zdroj (Sudety Mountains, SW Poland). *J Environ Radioact*, **46** (1): 121-129.

39. Li C, Su H, Zhang H, Zhou H (2016) Correlation between the spatial distribution of radon anomalies and fault activity in the northern margin of West Qinling Fault Zone, Central China. *J Radioanal Nucl Chem*, **308**: 679-686.

40. Srilatha MC, Rangaswamy DR, Sannappa J (2014) Studies on concentration of radon and physicochemical parameters in ground water around Ramanagara and Tumkur districts, Karnataka, India. *Int j adv sci tech res*, **4**(2): 641-660.